UNIVERSITY OF LEEDS

This is a repository copy of *Non-equilibrium processing of Ni-Si alloys at high undercooling and high cooling rates*.

White Rose Research Online URL for this paper:
http://eprints.whiterose.ac.uk/79861/

Version: Accepted Version

Article:

White Rose
university consortium
Universities of Leeds, Sheffield & York

eprints@whiterose.ac.uk
https://eprints.whiterose.ac.uk/

Non-Equilibrium Processing of Ni-Si Alloys at High Undercooling and High Cooling Rates

Andrew M Mullis[1,a], Leigang Cao[1,b] and Robert F Cochrane[1,c]

[1]Institute for Materials Research, University of Leeds, Leeds, LS2-9JT, UK.

[a]a.m.mullis@leeds.ac.uk, [b]pmlc@leeds.ac.uk, [c]r.f.cochrane@leeds.ac.uk

Abstract. Melt encasement (fluxing) and drop-tube techniques have been used to solidify a Ni-25 at.% Si alloy under conditions of high undercooling and high cooling rates respectively. During undercooling experiments a eutectic structure was observed, comprising alternating lamellae of single phase $\gamma(Ni_{31}Si_{12})$ and Ni-rich lamellae containing of a fine (200-400 nm) dispersion of β_1-Ni_3Si and α-Ni. This is contrary to the equilibrium phase diagram from which direct solidification to β-Ni_3Si would be expected for undercoolings in excess of 53 K. Conversely, during drop-tube experiments a fine (50 nm) lamellar structure comprising alternating lamellae of the metastable phase $Ni_{25}Si_9$ and β_1-Ni_3Si is observed. This is also thought to be the result of primary eutectic solidification. Both observations would be consistent with the formation of the high temperature form of the β-phase (β_2/β_3) being suppressed from the melt.

Introduction

Many intermetallics possess high hardness and good chemical stability at elevated temperature, making them ideal candidates for high temperature structural materials. However, a major obstacle to the utilisation of intermetallics is their lack of formability due to poor room temperature ductility. Potential routes to mitigate against this formability limitation include the incorporation of a ductile phase into the brittle intermetallic matrix and rapid solidification processing, whereby increased chemical disorder or a fine pattern of antiphase domains (APD's) increases ductility, making it less difficult to machine or forge to near net shape at room temperature. Upon subsequent annealing the chemical ordering, and hence the high temperature properties of the material, may be restored [1].

One such intermetallic is β-Ni_3Si, which displays excellent high temperature oxidation resistance, is generally resistant to corrosion in acid environments and has a yield strength which increases with temperature [2]. The focus of research on this material has been mainly on the microstructural evolution, as a function of undercooling, of the eutectic between α-Ni and β-Ni_3Si (Ni-21.4 at.% Si). Wei and Herlach [3] observed a gradual transition from lamellar to anomalous eutectic microstructure as the undercooling was increased, with the onset of the anomalous eutectic structure being observed at an undercooling of $\Delta T = 31$ K. The transition to the fully anomalous structure was complete at $\Delta T \sim 150$ K, with only the α-Ni and β-Ni_3Si phases being present. Leonhardt *et al.* [4], managed to achieve an increased undercooling level of 250K, wherein a double recalesence event could be observed. Moreover, by quenching the undercooled sample onto a chilled substrate the formation of metastable $Ni_{25}Si_9$ was observed. This metastable phase was also observed by Dutra *et al.* [5] using the melt-spinning technique.

The highest undercooling to be reported for this material was 550K by Lu *et al.* [6] and Liu *et al.* [7], using a combination of melt fluxing and cyclic superheating. With increasing undercooling the as-solidified microstructure displayed a complex evolutionary sequence from regular lamellar eutectic to anomalous eutectic, via intermediate structures including irregular lamellar eutectic, coarse directional dendritic, quasi-spherical eutectic colonies and fine directional dendritic. They also observed a significant refinement of the grain structure with increased undercooling, an observation common to many other deeply undercooled systems [8]. They attributed the observed grain refinement to enhanced nucleation, although many other mechanisms have been suggested to

account for this phenomenon in deeply undercooled melts, including post-recalescence remelting [9] and the development of growth instabilities [10, 11].

Recently Lu *et al*. [12] have extended their analysis to include Ni-29.8 at.% Si eutectic alloy, observing what they described as an interlaced morphology. They attributed this to the initial formation of γ ($Ni_{31}Si_{12}$) which subsequently remelted during recalescence to be replaced by an ordered δ-phase (Ni_2Si). At undercoolings in excess of 340 K [13] the microstructure showed a transition from a regular to a quasi-regular structure, which was attributed to the evolution from a faceted/faceted eutectic to a non-faceted/non-faceted eutectic.

In this paper the rapid solidification of a Ni-25 at.% Si alloy is investigated using both melt fluxing (high undercooling) and drop-tube (high cooling rate) methods to assess the feasibility of forming β-Ni_3Si direct from the melt. The equilibrium phase diagram for the Ni-rich end of the Ni-Si system [14] is shown in Fig. 1. Ni_3Si occurs in both low (β_1) and high (β_2/β_3) temperature forms, with these having the $L1_2$ and $D0_{22}$ crystal structures respectively. In addition, the high temperature phase has both an ordered and disordered form (β_2 and β_3 respectively), giving rise to the three forms shown in the phase diagram. The equilibrium solidification path from the melt for an alloy of initial composition around 25 at.% Si would be for the growth of γ-phase ($Ni_{31}Si_{12}$), with the subsequent conversion to β_3 via a peritectic reaction below 1443 K. With the γ-liquidus at this composition estimated at 1496 K direct access to β should become possible for undercoolings of ≈ 53 K or above.
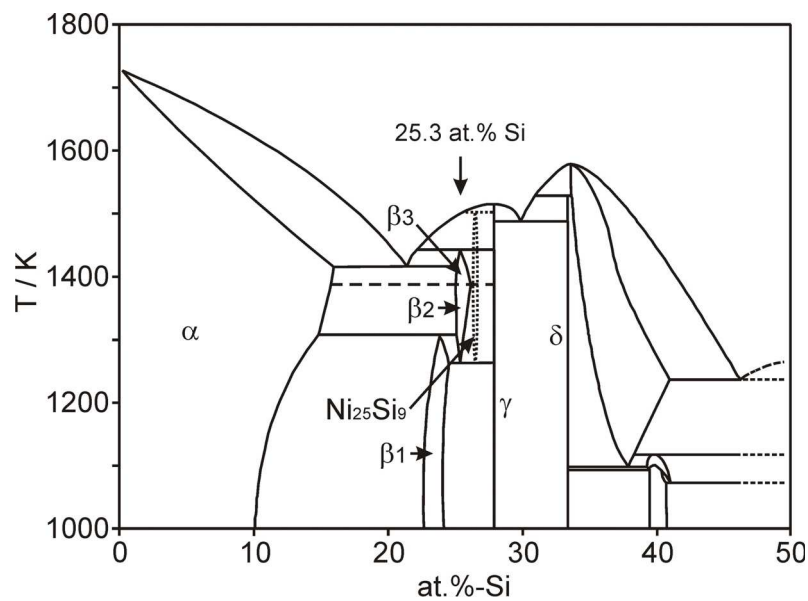

Fig. 1. Ni-rich portion of the Ni-Si equilibrium phase diagram, showing the 25.3 at.% Si composition studied in this work. Also shown is the location of the metastable $Ni_{25}Si_9$ phase, as determined by [4].

Experimental Method

A target composition of Ni-25.3 at.% Si was chosen as this corresponds to the region of the phase diagram over which the β_2/β_3 phase has the greatest temperature stability range (see Fig. 1). The alloy was produced by weighing and mixing elemental Ni and Si of 99.999% purity (metals basis) which were then formed into pellets by arc melting under an argon atmosphere. Arc melting of the pellets was repeated at least 10 times in order to ensure thorough mixing of the constituent elements. The pellets were weighed subsequent to arc melting to ensure no loss of material.

Undercooling experiments were performed within a stainless steel vacuum chamber evacuated to a pressure of 10^{-3} Pa using a turbo-molecular pump backed by a two stage, oil sealed, rotary vane pump. After being evacuated at this pressure for two hours the vacuum chamber was isolated from

the pumping system by means of a gate valve and backfilled to 50 kPa with N_2 gas. Samples were heated, in fused quartz crucibles, by induction heating of a graphite susceptor contained within an alumina shell, with temperature determination by means of an R-type thermocouple. Melt encasement, within a high purity flux, was employed to reduce the number of potential heterogeneous nucleation sites allowing the attainment of high undercoolings. Normally, for a material with a melting point > 1300 K a soda-lime glass flux would be used, however, due to a reaction between the soda-lime and the metal a B_2O_3 flux was used instead. Prior to performing the undercooling experiments the B_2O_3 flux was dehydrated for one hour by heating to just below its melting point under high vacuum. During a typical undercooling experiment the alloy would be superheated to 200 K above its melting point and, in order to achieve the highest undercoolings reported here, several heating-cooling cycles would be performed.

For drop-tube processing approximately 12 g of the alloy was loaded into an alumina crucible with three, 300 μm diameter, laser drilled holes in the base. This was then loaded into the drop tube furnace which was evacuated to $< 4.0 \times 10^{-3}$ Pa with a turbo-molecular pump before being backfilled with N_2 to 40 kPa. As with the undercooling experiments the sample was heated by induction of heating of a graphite susceptor, with temperature monitoring by means of an R-type thermocouple inside the melt crucible. When the desired superheat was achieved the sample was sprayed through the holes by pressuring the crucible with 0.4 MPa of N_2 gas. The resulting solidified powder was collected at the base of the drop-tube following a flight of approximately 6.5 m and sieved into standard size fractions.

Both flux undercooled and drop-tube samples were mounted in thermosetting transoptic resin, sectioned, ground on a series of progressively finer SiC papers and then polished using 6 μm, 3 μm and 1 μm diamond compounds. Microstructural analysis of the as-solidified samples was undertaken using an XL30 ESEM and Carl Zeiss EVO® MA 15 SEM.

Results

A maximum undercooling of $\Delta T = 160$ K was attained for this material by using cyclic fluxing and superheating. Upon nucleation a bright primary recalescence event was observed, which was followed in most cases by a much less bright secondary recalescence event. Following recalescence, the sample was allowed to cool at the ambient rate of the furnace, typically 2-5 K s^{-1}. Once cool, samples were removed from the glass flux for microstructural analysis.

The observed microstructure was similar at all undercoolings, displaying a lamellar structure characteristic of eutectic solidification. A typical example of this structure is shown in Fig. 2a for a sample undercooled by 80 K prior to nucleation. EBSD mapping reveals the lighter coloured lamellar to be γ-phase ($Ni_{31}Si_{12}$), while the darker lamellar are a Ni-rich phase for which we were not able to obtain an unambiguous indexing during EBSD mapping. A high resolution FEGSEM image of the same sample is shown in Fig. 2b. This confirms that the γ regions (top and bottom in Fig. 2b) are single phase, while the dark, Ni rich lamellar from Fig. 2a are shown to comprise a fine, two-phase dispersion. At yet higher magnification (TEM image, Fig. 2c) this two-phase region is shown to mostly comprise a continuous matrix of β_1-Ni_3Si containing isolated, sub-micron regions of α-Ni, although in the dark circular areas evident in Fig. 2b this structure is reversed. From the fine scale of the structure, and the observation of a second recalescence event in most undercooling experiments, we propose that the mixed α-β_1 structure is formed via a solid-state reaction subsequent to the primary solidification. In this model primary solidification would proceeded via a eutectic route giving alternating lamellar of γ-$Ni_{31}Si_{12}$ and a Ni-rich phase, possibly a supersaturated α solid solution. This Ni-rich phase would subsequently undergo a eutectoid decomposition to give the observed two phase structure in the Ni-rich lamellar.

With increasing undercooling only very minor changes in microstructure were observed, most notably some fragmentation of the γ lamellar and the presence of small amounts of both the metastable phase $Ni_{25}Si_9$ (< 3.3 % by volume) and the high temperature β_2/β_3-phase (< 4% by volume).

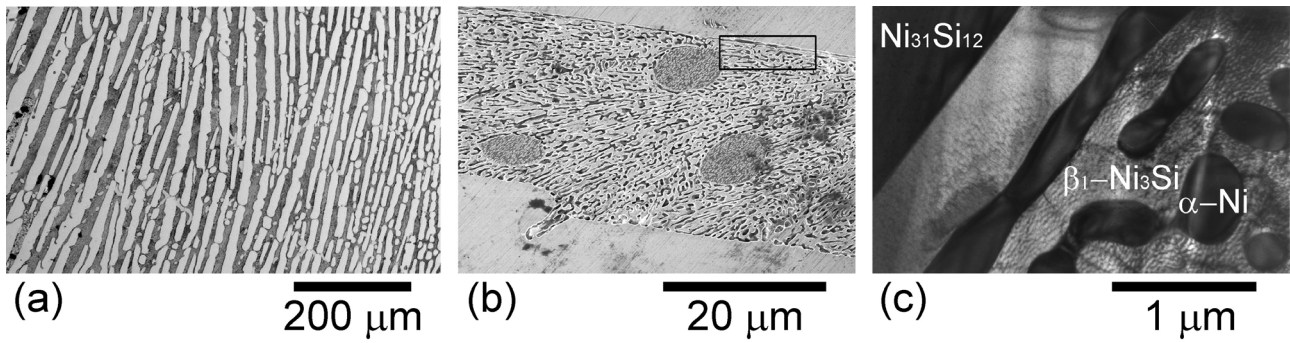(a)   200 µm   (b)   20 µm   (c)   1 µm

Ni₃₁Si₁₂

β₁–Ni₃Si   α–Ni

Fig. 2. Microstructure of an Ni-25.3 at.% Si alloy undercooled by 80 K prior to nucleation of solidification showing (a) lamellar structure of single phase γNi$_{31}$Si$_{12}$ (bright) and an Ni-rich phase (dark). At higher magnification (b & c) the Ni-rich lamellar are observed to consist of a sub-micron dispersion of β_1-Ni$_3$Si and α-Ni.

During drop-tube processing solidified particulates were produced with a diameter range of 500 – 100 µm. Contrary to flux processing, in which cooling rates are very low, cooling rates for the drop-tube particles are estimated from the model of Kasperovich *et al.* [15] to be 1300 – 10^4 K s^{-1}, for 500 µm to 100 µm droplets respectively. A typical droplet microstructure is shown in Fig. 3a, for a droplet in the 500 – 300 µm size range. In common with the flux undercooled samples we do not observe significant variations in the as-solidified structure between droplets, despite the very different cooling rates these are subject to. As with the flux undercooled samples the material shows a lamellar type structure characteristic of eutectic solidification, albeit at a much refined length scale, which is to be expected given the much higher cooling rates experienced in the drop-tube relative to the fluxing furnace. However, as shown in Fig. 3b, the resemblance to the structure of the flux undercooled samples is largely superficial, the majority phase now being the metastable Ni$_{25}$Si$_9$, with the minor phase being β_1-Ni$_3$Si. The formation of the metastable Ni$_{25}$Si$_9$ phase has been observed previously [4, 5], however the fine co-growth structure observed here has not been reported before. As can be seen from the phase diagram, there are two high temperature forms of β-phase, disordered β_3 and ordered β_2. However, XRD analysis failed to indicate the presence of either β_3 or β_2 in any drop-tube samples, although β_1 is identified both by XRD and by diffraction analysis in the TEM.
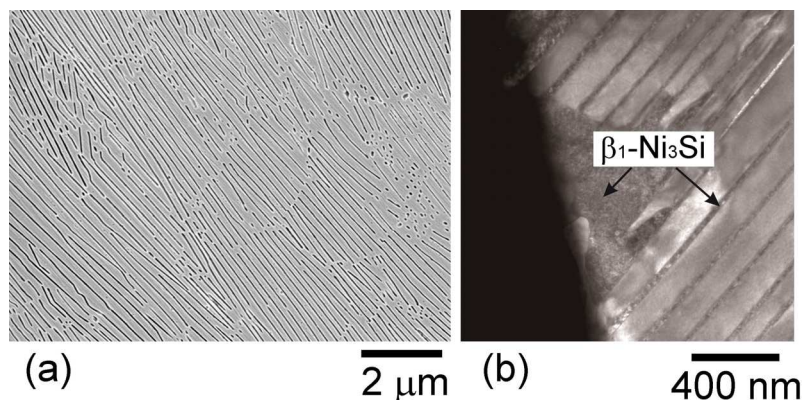

β₁-Ni₃Si

(a)   2 µm   (b)   400 nm

Fig. 3. Microstructure of a 500-300 µm diameter, drop-tube processed Ni-25.3 at.% Si droplet showing (a) eutectic like lamellar structure and (b) high resolution TEM image showing the very fine structure of the lamella. Diffraction analysis identifies the wide lamellar as Ni$_{25}$Si$_9$ and the thinner lamellar as β_1-Ni$_3$Si.

Discussion

The results presented above indicate that Ni-25 at.% Si has a least two non-equilibrium solidification pathways. The phase diagram suggest that for undercoolings of 53 K $\leq \Delta T \leq$ 108 K direct access to the high temperature form of β-phase (β_2/β_3) should be possible, although this is not observed experimentally. At low cooling rate the direct formation of β-phase from the liquid appears to be inhibited and instead solidification proceeds via a metastable eutectic between a γ-$Ni_{31}Si_{12}$ and a Ni-rich phase, with the subsequent eutectoid decomposition of the Ni-rich phase to α-Ni and β_1-Ni_3Si. Conversely, at high cooling rates an alternative lamellar structure, consisting of very fine alternating lamellar of $Ni_{25}Si_9$ and β_1-Ni_3Si, is observed. One possible formation route to this structure may be the direct solidification to, and subsequent solid-state decomposition of, β_2/β_3-Ni_3Si. Certainly the near 100 fold reduction in the characteristic length scale of the microstructure between the slowly cooled (fluxed) samples and rapidly cooled (drop-tube) samples would be consistent with this morphology resulting from an eutectoid reaction. However, there is no evidence of any β_2/β_3 being retained in the drop-tube samples, despite the presence of up to 4% β_2/β_3 being retained in the highly undercooled flux samples, which experience much lower cooling rates than those encountered in the drop-tube. It is therefore also possible that the observed $Ni_{25}Si_9$ - β_1 lamellar are the primary solidification morphology and that this represents a second, and previously unobserved, metastable eutectic reaction. In this case the very fine scale of the microstructure would be indicative for very low diffusivity in the liquid, circumstantial evidence for which is discussed below.

We suggest that the observed solidification morphologies may result from a difficulty in nucleating solidification of the β_2/β_3-phase from the melt. Similar behaviour has been observed in Nb- xSi (x = 21.0 - 27.0 at.%) alloys, where for undercoolings in excess of 270 K (based on the equilibrium phase-diagram) direct solidification to primary Nb_3Si should be observed. However, Bertero et al. [16] found that in levitated drops of these alloys, primary solidification was to a metastable α-Nb + β-Nb_5Si_3 eutectic, an observation they attributed to difficulty in nucleating the Nb_3Si phase. Such inhibition of nucleation could potentially be explained by a mismatch between the crystal structure of the equilibrium solid and any short range order present in the (undercooled) liquid. CALPHAD modelling of the Ni-Si binary system reveals that if formation of β-phase is suppressed, the equilibrium solidification pathway for a Ni-25 at.% Si alloy would be the formation of an α-γ eutectic. We therefore suggest that the solidification pathway for this material is primary eutectic solidification to γ-$Ni_{31}Si_{12}$ and supersaturated α-Ni solid-solution, with the subsequent eutectoid decomposition to the supersaturated solid-solution to give the observed fine two-phase dispersion of α-Ni and β_1-Ni_3Si. Moreover, Ahmad et al., [17] have shown that solidification velocities in this alloy are exceptionally low, typically < 0.02 m s^{-1} for the highest undercoolings reported here, indicating very low atomic mobility in the melt, which may explain why during rapid cooling $Ni_{25}Si_9$ (26.4 at% Si), which is closer in composition to the melt than γ-$Ni_{31}Si_{12}$ (27.9 at.% Si), is the preferred solid to be formed.

References

[1] R. W. Cahn, P. A. Siemers, J. E. Geiger and P. Bardham, The order-disorder transformation in Ni_3Al and Ni_3Al-fe alloys: 1. Determination of the transition-temperatures and their relation to ductility, Acta Metall. 35 (1987) 2737.

[2] P. H. Thornton and R. G. Davies, Temperature dependence of flow stress of gamma prime phases having L_{12} structure, Metall. Trans. 1 (1970) 549.

[3] B. Wei and D.M. Herlach, Rapid solidification of bulk undercooled Ni-21.4 at %Si eutectic alloy, Trans. Mat. Res. Soc. Jpn. 14A (1995) 639.

[4] M. Leonhardt, W. Loser and H. G. Lindenkreuz, Metastable phase formation in undercooled eutectic $Ni_{78.6}$ $Si_{21.4}$ melts, Mater. Sci. Eng. A 271 (1999) 31-37.

[5] A. T. Dutra, S. Milenkovic, C. S. Kiminami, A. M. Santino, M. C. Goncalves and R. Caram, Microstructure and metastalble phase formation in a rapidly solidified Ni-Si eutectic alloy using a melt-spinning technique, J. Alloys Compounds 381 (2004) 72.

[6] Y. P Lu, F. Liu, G.C Yang, H. P. Wang and Y. H. Zhou, Grain refinement in solidification of highly undercooled eutectic Ni-Si alloy, Mater. Lett. 61 (2007) 987.

[7] F. Liu, Y. Z. Chen, G. C. Yang, Y. P. Lu, Z. Chen and Y. H. Zhou, Competitions incorporated in rapid solidification of the bulk undercooled eutectic $Ni_{78.6}$ $Si_{21.4}$ alloy, J. Mater. Res. 22 (2007) 2953.

[8] S. E. Battersby, R. F. Cochrane and A. M. Mullis, Highly undercooled germanium: Growth velocity measurements and microstructural analysis, Mater. Sci. Eng. A 226 (1997) 443.

[9] M. Schwarz, A. Karma, K. Eckler and D. M. Herlach, Physical-mechanism of grain-refinement in solidification of undercooled melts, Phys. Rev. Lett. 73 (1994) 1380.

[10] A. M. Mullis and R. F. Cochrane, Grain refinement and the stability of dendrites growing into undercooled pure metals and alloys, J. Appl. Phys. 82 (1997) 3783.

[11] A. M. Mullis, Rapid solidification within the framework of a hyperbolic conduction model, Int. J. Heat Mass Transf. 40 (1997) 4085.

[12] Y. P. Lu, F. Liu, G. C. Yang and Y. H. Zhou, Composite growth in highly undercooled $Ni_{70.2}$ $Si_{29.8}$ eutectic alloy, App. Phys. Lett. 89 (2006) 241902.

[13] Y. P. Lu, X. Lin, G. C. Yang, J. Li and Y. H. Zhou, The formation of quasiregular microstructure in highly undercooled $Ni_{70.2}$ $Si_{29.8}$ eutectic alloy, J. Appl. Phys. 104 (2008) 013535.

[14] T. B. Massalski, P. R. Subramanian, H. Okamoto and L. Kacprzak. Binary Alloy Phase Diagrams, 2nd ed. ASM International, Materials Park, OH, 1990.

[15] G. Kasperovich, T. Volkman, L. Ratke and D. Herlach, Microsegregation during solidification of an Al-Cu binary alloy at largely different cooling rates (0.01 to 20,000 K/s): Modeling and experimental study, Metall. Mater. Trans. A 39 (2008) 1183.

[16] G. A. Bertero, W. H. Hofmeister, M. B. Robinson and R. J. Bayuzick, Containerless processing and rapid solidification of Nb-Si alloys of hypereutectic composition, Metall. Trans. A 22 (1991) 2723.

[17] R. Ahmad, R. F. Cochrane and A. M. Mullis, The formation of regular αNi-γ ($Ni_{31}Si_{12}$) eutectic structures from undercooled Ni-25 at.% Si melts, Intermetallics 22 (2012) 55.